# Stator-Flux-Oriented Control with High Torque Dynamics for IM and PMSM

M. Spichartz, M. Oettmeier, C. Heising, V. Staudt and A. Steimel
Ruhr-University Bochum
D-44780 Bochum
Germany
Tel.: +49 234 32 23890
Fax.: +49 234 32 14597
Email: spichartz@eele.rub.de, oettmeier@eele.rub.de, heising@eele.rub.de, staudt@eele.rub.de, steimel@eele.rub.de

***Abstract*— Electric vehicles pose specific challenges to the drive system and the control scheme. Safety-relevant features like slip-slide control, electronic stability programs or emergency-brake assistance require fast torque control in the whole speed range at limited voltage control margin.**

**Stator-flux-oriented Indirect Stator-Quantities Control (ISC) is limited only by the physical bounds of available voltage and switching frequency and allows special guidance of the flux trajectory to reach excellent torque performance.**

**In this paper, ISC is introduced for the induction machine as well as for the permanent-magnet synchronous machine. Torque transients are presented for both machine types in comparable dimensioning.**

## I. Introduction

Stator-flux-oriented Indirect Stator-Quantities Control (ISC) satisfies the high requirements for the drive system of electric-vehicle (EV) applications with excellent performance. ISC is in practical use in many railway applications, especially for feeding induction machines (IM). The torque dynamic is limited only by the physical bounds of available voltage and switching frequency. Moreover, it does not require any voltage control margin in field-weakening range.

The benefits of the stator-flux oriented control can be transfered to EV applications. The high torque at low speed combined with very high maximum speed force a wide field-weakening range. Therewith the voltage control margin is limited in a wide operation range. In spite of the strictly limited control margin, ISC allows highest torque dynamics. This is a basic demand for safety-relevant features like slip-slide control, electronic stability programs or emergency-brake assistance that require fast torque control in the whole speed range.

The stator-flux orientation can be applied for permanent-magnet synchronous machines (PMSM) as well.

In this paper a typical structure of an EV power train is presented. The stator-flux-oriented approach is introduced briefly and ISC as PWM-based stator-flux-oriented control for induction machines is presented in detail. The differences to PMSM control are suggested. The abilities are illustrated using simulation of torque-step responses for both machines. IM and PMSM used in the simulation scenario are dimensioned for use in an electric vehicle (cf. table I). The quality of the simulation is verified by measurement results at a laboratory test set-up with a railway-traction IM controlled by ISC.

## II. Power train

A modern drive for EV consists of a three-phase two-level inverter feeding a rotating-field machine (Fig. 1). The machine is connected to the mechanical power train of the vehicle.

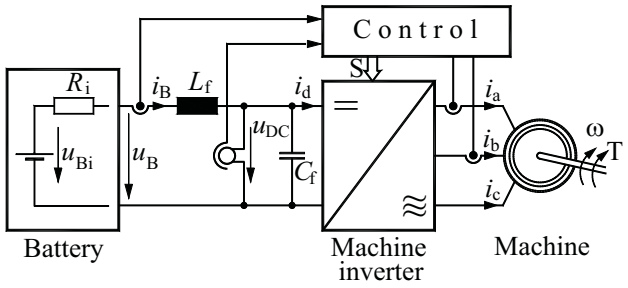


Fig. 1. Structure of EV drive system

In contrast to electric drives in traction and industrial use, the inverter is not connected to a constant-voltage-controlled DC link with a large capacitor. A battery acts as energy source and is linked by a second-order LC-filter ($L_f$,$C_f$) to the inverter. The filter reduces the distortion current and avoids thermal overloading of the battery.

Due to space restrictions, the filter capacitor is small. Furthermore, the internal resistance of the battery source and the ohmic resistance of the wiring let the DC voltage $u_{DC}$ vary as a consequence of the charging level and of the load current resulting from acceleration or deceleration.

The power train of an EV drive poses specific demands to the dimensioning and the control of the machine. State-of-the-art is the use of induction machines or permanent-magnet synchronous machines.

In the following, the attention is focussed on the control of the rotating-field machine, not on the discussion of the respective benefits or drawbacks using IM or PMSM [1]–[3]. As a first approximation the internal resistance of the battery is neglected ($u_{DC} = const.$).

978-1-4244-8218-4/10/$26.00 ©2010 IEEE

The models of the machines are presented to define all electrical parameters and flux linkages.

## III. Induction machine

For stator-flux orientation the canonical Γ-equivalent circuit diagram (ECD) of the induction machine, using the stator-fixed reference system ($\omega_B = 0$), is most adequate (Fig. 2). Space-vector (SV) notation is used for description, denoted by arrows under the letter symbols.

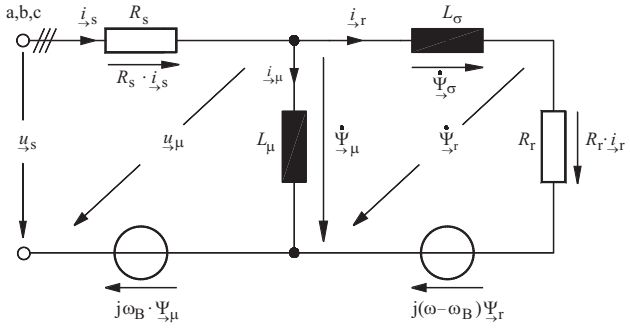


Fig. 2. Equivalent circuit diagram of induction machine in space-vector notation

The rotor has the electrical angular velocity $\omega = 2\pi\, n\, p$ with rotor speed $n$ and number of pole pairs $p$. Rotor and stator angular velocity differ by the angular rotor frequency $\omega_r$ and the time-derivative of the angle $\vartheta$ between stator- and rotor-flux SVs, in the dynamic case.

$$\omega_s = \omega + \omega_r + \dot{\vartheta} \tag{1}$$

The derivative of the flux space vectors can be read off the equivalent circuit diagram as:

$$\dot{\underrightarrow{\Psi}}_\mu = \underrightarrow{u}_s - R_s \underrightarrow{i}_s - j\omega_B \underrightarrow{\Psi}_\mu \tag{2}$$

$$\dot{\underrightarrow{\Psi}}_r = R_r \underrightarrow{i}_r + j(\omega - \omega_B)\underrightarrow{\Psi}_r \tag{3}$$

With the state-space model the induction machine is described correctly in the stationary as well as in the dynamic case.

$$\begin{pmatrix} \dot{\underrightarrow{\Psi}}_\mu \\ \dot{\underrightarrow{\Psi}}_r \end{pmatrix} = \begin{pmatrix} -R_s \dfrac{L_\mu + L_\sigma}{L_\mu \cdot L_\sigma} - j\omega_B & \dfrac{R_s}{L_\sigma} \\ \dfrac{R_r}{L_\sigma} & -\dfrac{R_r}{L_\sigma} + j\,(\omega - \omega_B) \end{pmatrix} \cdot \begin{pmatrix} \underrightarrow{\Psi}_\mu \\ \underrightarrow{\Psi}_r \end{pmatrix} + \begin{pmatrix} \underrightarrow{u}_s \\ 0 \end{pmatrix} \tag{4}$$

$$\underrightarrow{i}_s = \underrightarrow{i}_\mu + \underrightarrow{i}_r = \begin{pmatrix} \dfrac{L_\mu + L_\sigma}{L_\mu \cdot L_\sigma} & -\dfrac{1}{L_\sigma} \end{pmatrix} \cdot \begin{pmatrix} \underrightarrow{\Psi}_\mu \\ \underrightarrow{\Psi}_r \end{pmatrix} \tag{5}$$

Torque can be calculated in two different ways:

$$T = \frac{3}{2} \cdot p \cdot \mathrm{Im}\left\{ \underrightarrow{\Psi}_\mu^* \cdot \underrightarrow{i}_s \right\} \tag{6}$$

$$T = \frac{3}{2} \cdot p \cdot \frac{1}{L_\sigma} \cdot \left| \underrightarrow{\Psi}_\mu \right| \cdot \left| \underrightarrow{\Psi}_r \right| \cdot \sin(\vartheta) \tag{7}$$

with $\vartheta = \chi(\underrightarrow{\Psi}_\mu) - \chi(\underrightarrow{\Psi}_r)$.

The modulus of the rated stator-flux SV is given as

$$\Psi_\mu^* = \left| \underrightarrow{\Psi}_{\mu,rated} \right| = \sqrt{\frac{2}{3}} \cdot \frac{U_{s,rated}}{2\pi f_{s0}} \tag{8}$$

This delivers the breakdown torque at rated stator-flux in the voltage-control range of the machine.

$$T_{br} = \frac{3}{4} \cdot p \cdot \frac{\Psi_\mu^{*2}}{L_\sigma} \tag{9}$$

In the field-weakening range the breakdown torque $T_b$ decreases quadratically with the weakening of the stator flux.

## IV. Permanent-magnet synchronous machine

Whilst the symmetrical (isotropic, non-salient-pole rotor) synchronous machine can be suitably represented by an $\alpha, \beta$-coordinate system for stator-flux control, a transformation of the quantities into a dq-coordinate system associated with the pole position is necessary to model the anisotropic synchronous machine (permanent-magnet salient-pole machine of IPM type).

The three components a, b, c will be first converted into space vector $\alpha, \beta$-coordinates in the stator-winding-fixed reference frame:

$$\underrightarrow{x}^{\alpha\beta} = \begin{bmatrix} x_\alpha \\ x_\beta \end{bmatrix} = \frac{2}{3} \begin{bmatrix} 1 & -\frac{1}{2} & -\frac{1}{2} \\ 0 & \frac{\sqrt{3}}{2} & -\frac{\sqrt{3}}{2} \end{bmatrix} \begin{bmatrix} x_a \\ x_b \\ x_c \end{bmatrix} \tag{10}$$

Subsequently, they are converted by means of the Park Transformation to the rotor-fixed reference frame; the angle between stator reference and rotor reference is $\gamma$.

$$\underrightarrow{x}^{dq} = \begin{bmatrix} x_d \\ x_q \end{bmatrix} = \begin{bmatrix} \cos\gamma & \sin\gamma \\ -\sin\gamma & \cos\gamma \end{bmatrix} \begin{bmatrix} x_\alpha \\ x_\beta \end{bmatrix} = \underrightarrow{x}^{\alpha\beta} \cdot e^{-j\gamma} \tag{11}$$

Fig. 3 shows the standard ECD for the anisotropic PMSM. Typically, no iron losses are included. Furthermore, the flux is aligned to the d axis, so that the flux in q direction is zero: $\Psi_{Eq} = 0$. The stator-flux SV $\underrightarrow{\Psi}_S$ is described by its d- and q-components ($\Psi_d$ and $\Psi_q$) [4].

In component notation, the differential equations are as follows [5]:

$$\dot{\Psi}_d = u_d - R_s i_d + \omega \Psi_q \tag{12}$$

$$\dot{\Psi}_q = u_q - R_s i_q - \omega \Psi_d \tag{13}$$

$$\Psi_d = \Psi_E - L_d i_d \tag{14}$$

$$\Psi_q = L_q i_q \tag{15}$$

$$M_d = \frac{3}{2} p \left[ \Psi_E \cdot i_q + (L_d - L_q)\, i_d i_q \right] \tag{16}$$

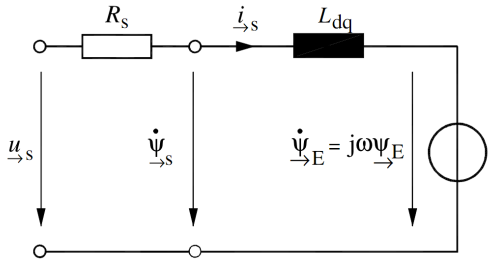


Fig. 3. Space-vector ECD of anisotropic PMSM

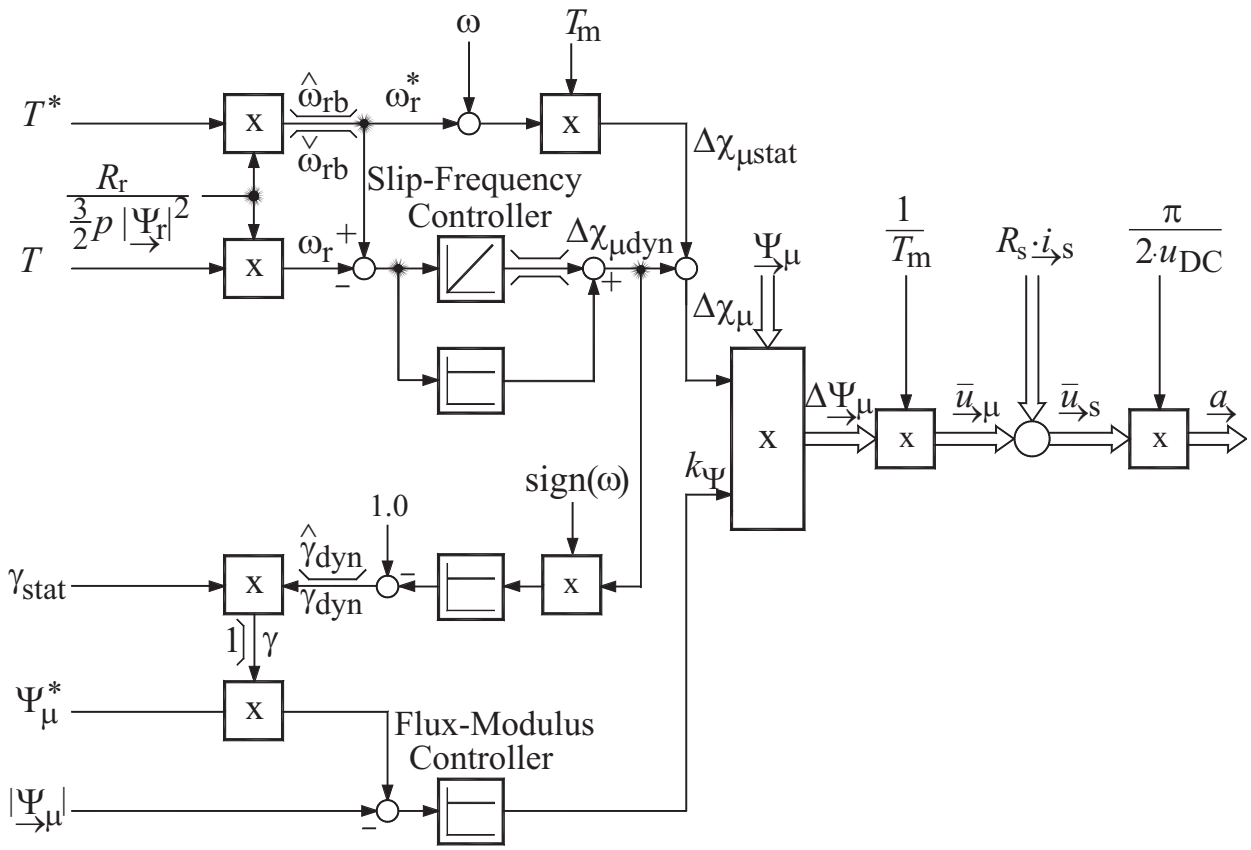


Fig. 4. Structure of Indirect Stator-Quantities Control of induction machines

## V. Stator-flux-oriented control of rotating-field machines

Stator-flux-oriented control schemes guide the tip of the stator-flux SV on a predetermined trajectory, in general a non-regular multi-corner polygon. By accelerating or slowing down the stator-flux SV the demanded torque is produced with highest dynamic. Furthermore the modulus of the stator-flux SV is always kept close to the reference value independent of the working point and torque demands.

In the case of high switching frequency, the polygon is converging to a circle concentric to the origin. For low switching frequencies – for example in traction drives – non-PWM-based control schemes are used that replace the circle by a regular hexagon or a 18-corner figure [6].

The special guidance is of benefit to reach highest dynamic with lowest voltage margin in the field-weakening range [7], too. The ISC is a PWM-based control that takes full advantage of the benefit of stator-flux orientation in voltage-control as well as in field-weakening range.

The concept of ISC has originally been developed to control induction machines. The radius of the ideally circular trajectory is defined by controlling the modulus of the stator-flux SV. By switching the accurate stator-voltage SV mean value per modulation period $T_m$, the movement of the stator-flux SV will be accelerated or slowed down in relation to the rotor-flux SV in the next modulation period. This causes an angle $\vartheta$ between the stator- and rotor-flux SVs, hence producing the demanded torque. Details are given in [8]–[10].

This main principal control concept of ISC can also be used for a stator-flux-oriented control of PMSM. The stator-flux SV $\underrightarrow{\Psi}_S$, which is obtained from the usually optimized d- and q-components [4], [11] as $\sqrt{\Psi_d^2 + \Psi_q^2}$ with the angle $\zeta$ to the d-axis, is directly controlled as well and can be guided on a well-directed trajectory in relation to the excitation-flux SV $\underrightarrow{\Psi}_E$.

The differences between d-axis inductivity and q-axis inductivity, due to the anisotropic construction of IPMSM, as well as saturation are not negligible and influence the torque behaviour in a complex way.

In the following the structure of ISC for induction machines is presented in detail. Main differences for PMSM control are suggested.

The controller is divided into a torque and a stator-flux-modulus controller. Fig. 4 shows the two-parted structure of the controller [9]. The stator-flux modulus is controlled by a P-type Flux-Modulus Controller via $k_\Psi$. The angle increment $\Delta\chi_\mu$ is controlled then by the Slip-Frequency Controller.

Torque set and actual values are first transformed to rotor (slip) angular frequencies. Thus breakdown can easily be prevented by limiting the modulus of the set value to the value of the rotor breakdown angular frequency $\omega_{rb}$ [8], [10].

The two controllers calculate the stator-flux increment

$\Delta\underrightarrow{\Psi}_\mu$ to move the stator-flux SV between the beginning $(\nu-1)$ and the end $(\nu)$ of a modulation period (Fig. 5). In the most general case, the stator-flux SV is 'stretched' to the flux set-point value and rotated by $\Delta\chi_\mu(\nu)$ depending on rotor angular velocity, torque and derivative of the angle $\vartheta$.

The stator-flux increment $\Delta\underrightarrow{\Psi}_\mu$ divided by the modulation period $T_m$ yields the necessary inner motor voltage, which – increased by the stator-resistance voltage drop and normalized to $\frac{2}{\pi}u_{DC}$ – is handed as voltage control factor SV (VCF) $\underrightarrow{a}$ to the PWM control of the inverter (Fig. 4). There are no subordinated current-component controllers anymore.

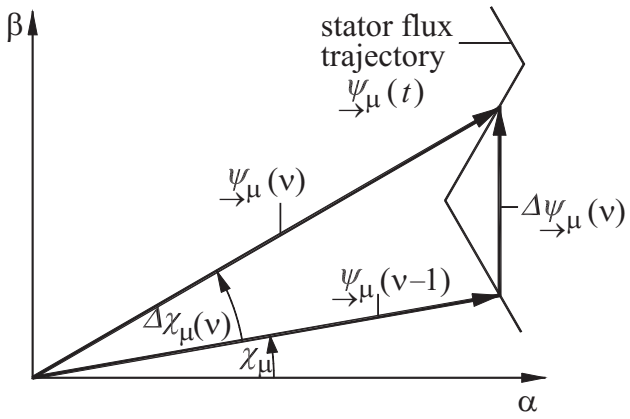


Fig. 5. Stator-flux trajectory and stator-flux increment per modulation period $T_m$

In stationary operation a feed-forward control for the slip-frequency controller is used. The stationary angle increment $\Delta\chi_{\mu,stat}$ is calculated from measured and reference (index *) quantities:

$$\Delta\chi_{\mu,stat} = \omega_s^* \cdot T_m = (\omega + \omega_r^*) \cdot T_m \qquad (17)$$

The stationary operation of the feed-forward control is stable and does not show any control deviation. Based on an exact quasi-instantaneous machine observer the angle increment $\Delta\chi_{\mu,dyn}$ of the slip-frequency controller is nil in stationary operation. This relieves the PI controller in dynamic situations. The integral contribution can be limited to a small value; it is provided only to prevent stationary control error. In dynamics the controller has almost exclusively a proportional part. Thus there is no overshoot after a torque step.

The torque control for PMSM is simplified by the known rotor position and therewith the knowledge of the instantaneous value of the excitation-flux SV $\underrightarrow{\Psi}_E$. The slip-frequency controller is replaced by a torque controller that calculates the necessary stator-flux increment $\Delta\underrightarrow{\Psi}_\mu$ depending on the set-point value.

To use ISC in the operating range of high stator frequencies, the controller enables field-weakening operation [7]. The field-weakening factor $\gamma$ is defined as the product of a stationary and a dynamic part:

$$\gamma = \gamma_{stat} \cdot \gamma_{dyn} = \frac{\Psi^*_{\mu,weak}}{\Psi^*_\mu} \qquad (18)$$

The stationary field-weakening factor $\gamma_{stat}$ is calculated so that the maximum VCF is used for any stator frequency in the field-weakening range, without any voltage margin in stationary operation.

To achieve good dynamics without voltage margin the stretch factor $k_\Psi$ is reduced for torque dynamics. That shortens the stator-flux SV trajectory and the stator-flux SV is accelerated in comparison to the rotor-flux SV by the shorter track length [8]–[10].

A dynamic field-weakening factor $\gamma_{dyn}$ is defined, depending on the demand of the slip-frequency controller. The dynamic field-weakening is calculated by a simple P-controller, the complex trajectory does not have to be precalculated. It is already activated at the end of the voltage-control range, to keep highest torque dynamic even though the voltage control margin decreases to zero.

## VI. Simulation Results

### A. Simulation concept and verification

The power train is analysed and modelled by a simulation programmed in 'C++' language [12].

The quality of the simulation is verified by comparison to measurements. As the dimensioned machines do not exist physically, the measurements are performed using a drive test bench for railway application with a three-phase two-level converter feeding an induction machine ($P_{rated} = 120\,\mathrm{kW}$, $n_0 = 1200\,\mathrm{min}^{-1}$). The induction machine is torque-controlled by ISC and coupled with a speed-controlled separately-excited DC machine [8], [9].

Fig. 6 and 7 show the stator currents $i_{sa}$ and $i_{sc}$ of the induction machine at $n = 1000\,\mathrm{min}^{-1}$ at no-load and at motor operation ($T/T_{br} = 0.2$). The measurement and simulation results are plotted among each other.

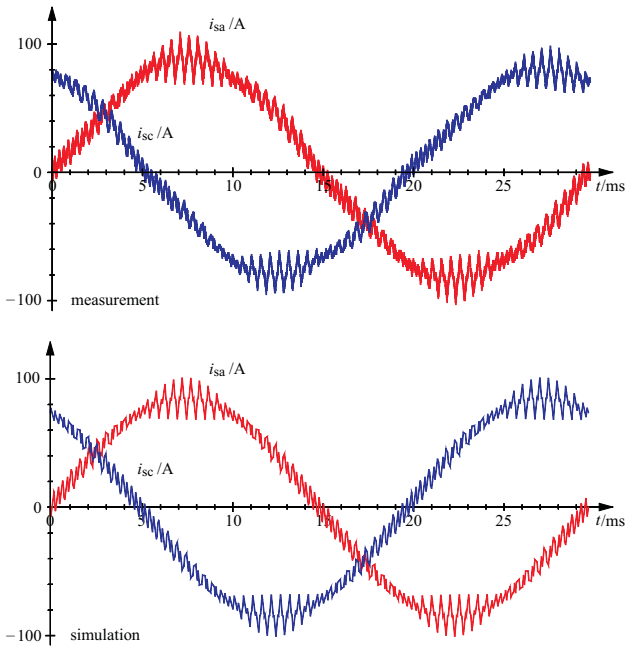


Fig. 6. Comparison of measurement and simulation of ISC-controlled IM; $n = 1000\,\mathrm{min}^{-1}$ and no-load

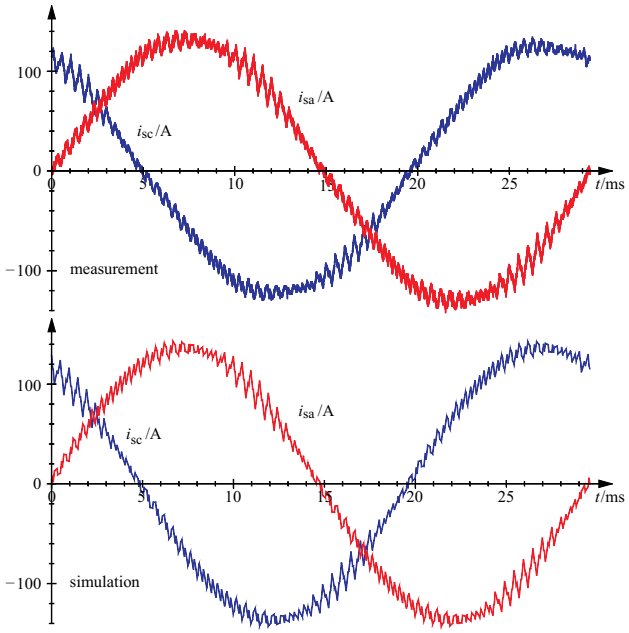


Fig. 7. Comparison of measurement and simulation of ISC-controlled IM; $n = 1000\,\mathrm{min}^{-1}$ and $T/T_{br} = 0.2$

The used simulation shows excellent results in comparison with measurements and its accuracy is so high [13], that all following time-domain analysis is done by simulation.

In the following simulations the excellent stationary and dynamic torque behaviour of ISC in voltage-control range is presented for EV-specific dimensioned IM and PMSM. The analysis of the flux trajectories in voltage-contol range and field-weakening range are not in the scope of this paper. Details are given in [7].

### *B. Simulation results of ISC-controlled IM and PMSM*

Fig. 8 and 9 show simulation results of IM and PMSM controlled by the introduced stator-flux-oriented control. To demonstrate the performance of this control concept, the set-point value of torque is changed abruptly from 0 to $120\,\mathrm{Nm}$ at $t = 8\,\mathrm{ms}$, changing the operation mode of the machines from no-load to motor operation and from motor operation to braking ($-120\,\mathrm{Nm}$) at $t = 58\,\mathrm{ms}$. The set-point of torque is set back to no-load at $t = 108\,\mathrm{ms}$. The figures display the stator current $i_{sa}$, the desired set-point of the torque $T^*$ and the actual torque $T$. In addition to these quantities the simulation of the PMSM shows the actual orientation angle $\chi$ of the rotor. The switching frequency is $f_c = 2\,\mathrm{kHz}$.

The zoom which is provided for each simulation shows the transient behaviour of the control in case of the change between motor operation and braking. It can be seen that steady-state is obtained within less than $1\,\mathrm{ms}$ for both types of machines.

## VII. Conclusions

The stator-flux-oriented ISC fulfills the EV-specific demands of high performance and robustness.

The successful application of ISC for induction machines in railway traction is easily and successfully transferable to EV applications. The torque dynamic in the whole operation range is very high and can be used for high-performance control features like slip-slide control, electronic stability programs or emergency brake assistance.

Furthermore this control scheme can also be used for stator-flux-oriented control of PMSM with comparable results.

TABLE I
Machine Data

| | IM | PMSM |
|---|---|---|
| $P_{rated}$ | $22\,\mathrm{kW}$ | $22\,\mathrm{kW}$ |
| $U_{s,rated}$ | $148\,\mathrm{V}$ | $148\,\mathrm{V}$ |
| $I_{s,rated}$ | $330\,\mathrm{A}$ | $330\,\mathrm{A}$ |
| $T_{rated}$ | $233\,\mathrm{Nm}$ | $233\,\mathrm{Nm}$ |
| $p$ | 3 | 6 |
| $n_{rated}$ | $900\,\mathrm{min}^{-1}$ | $900\,\mathrm{min}^{-1}$ |
| $n_{max}$ | $7200\,\mathrm{min}^{-1}$ | $7200\,\mathrm{min}^{-1}$ |

## References


[1] Ehsani, M. amd Gao, Y. and Gay, S., "Characterization of electric motor drives for traction applications," in *The 29th Annual Conference of the IEEE Industrial Electronics Society (IECON '03)*, (Roanoke, Virginia, USA), pp. pp. 891 – 896, 2003.

[2] S. Williamson, A. Emadi, and K. Rajashekara, "Comprehensive efficiency modeling of electric traction motor drives for hybrid electric vehicle propulsion applications," *IEEE Transactions on Vehicular Technology*, vol. 56, no. 4, pp. 1561 – 1572.

[3] K. Rahman and M. Ehsani, "Performance analysis of electric motor drives for electric and hybrid electric vehicle applications," *IEEE Power Electronics in Transportation*, pp. 49 – 56, 1996.

[4] T. M. Jahns, "Flux-weakening regime operation of an interior permanent-magnet synchronous motor drive," *IEEE Transactions on Industry Applications*, vol. 23, pp. 681–689, 1987.

[5] D. Schroeder, *Elektrische Antriebe - Regelung von Antriebssystemen, 3. Auflage*. Springer-Verlag Berlin-Heidelberg, 2009.

[6] U. Baader, "Hochdynamische Drehmomentregelung einer Asynchronmaschine im ständerflussbezogenen Koordinatensystem," in *EtzArchiv 6*, pp. 11–16, 1989. H. 1.

[7] M. Spichartz, C. Heising, V. Staudt, and A. Steimel, "Indirect Stator-Quantities Control as Benchmark for Highly Dynamic Induction Machine Control in the Full Operating Range," in *14th International Power Electronics and Motion Control Conference (EPE-PEMC)*, (Ohrid, Republic of Macedonia), 2010.

[8] M. Jänecke and F. Hoffmann, "Fast Torque Control of an IGBT-Inverter-Fed Three-Phase A.C. Drive in the Whole Speed Range - Experimental Results," in *6th Europ. Conf. on Power Electronics, Vol. 3*, (Sevilla), pp. 399–404, 1995.

[9] M. Depenbrock, C. Foerth, F. Hoffmann, S. Koch, A. Steimel, and M. Weidauer, "Speed-sensorless stator-flux-oriented control of induction motor drives in traction," *Communications - Scientific Letters of the University of Zilina*, vol. 2-3, pp. 68–75, 2001.

[10] D. Maischak and M. Nemeth-Czoka, "Schnelle Drehmomentregelung im gesamten Drehzahlbereich eines hochausgenutzten Drehfeldantriebs," in *Archiv für Elektrotechnik 77*, pp. 289–301, 1994.

[11] J. Fang, C. Heising, V. Staudt, and A. Steimel, "Permanent-Magnet Synchronous Machine Model for Urban Transport Applications," in *12th International Conference on Optimization of Electrical and Electronic Equipment (OPTIM)*, (Brasov, Romania), 2010.

[12] C. Heising, R. Bartelt, M. Oettmeier, V. Staudt, and A. Steimel, "Simulation tool for coupled but independently controlled power-electronic systems applied to npc converters," in *Power Conversion Intelligent Motion (PCIM)*, (Nuremberg), 2010.

[13] V. Staudt, C. Heising, and A. Steimel, "Advanced simulation concept for power train of loco and its verification," in *ICPE 07 Conference*, (Daegu, South Korea), 2007.

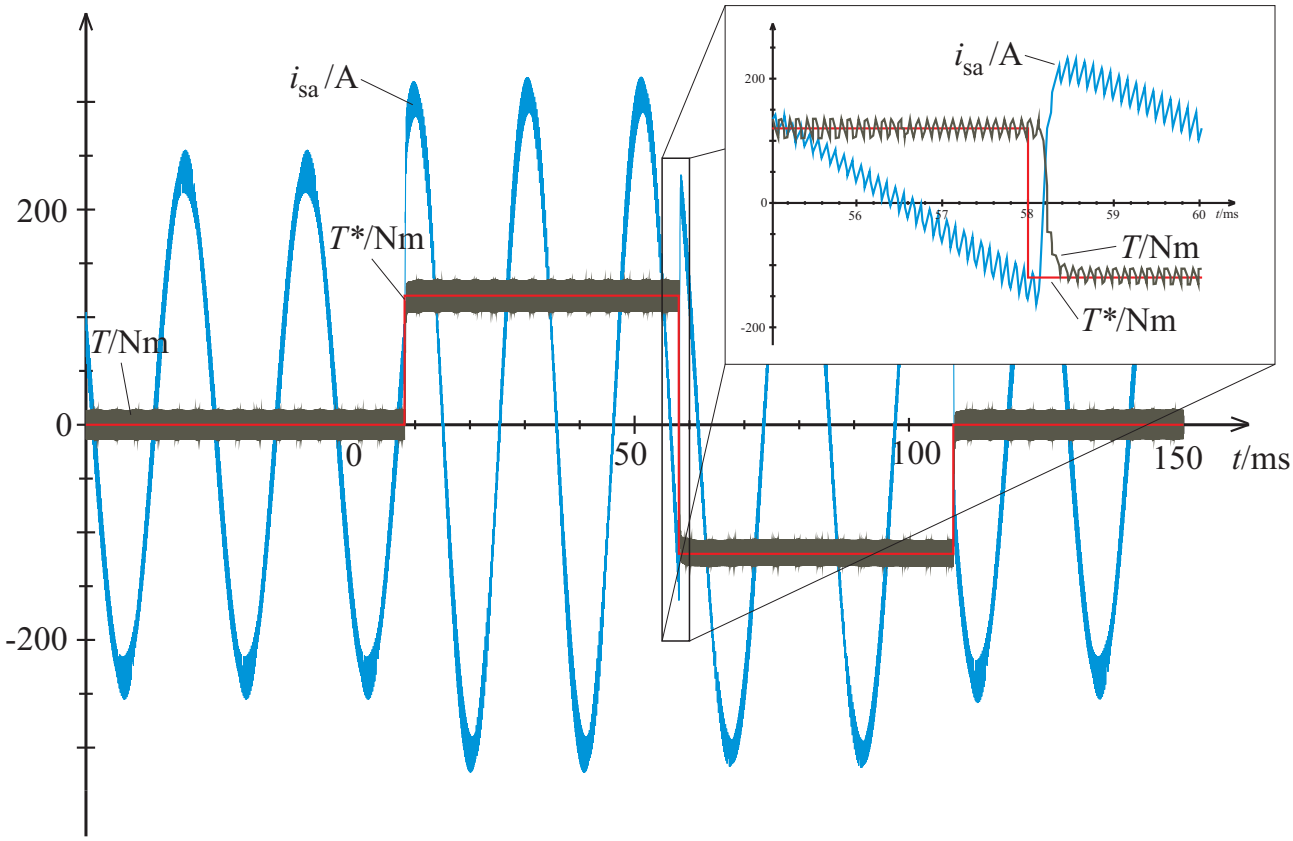


Fig. 8. Torque steps of ISC-controlled IM at $n = 900\,\mathrm{min}^{-1}$; $u_{DC} = 200\,\mathrm{V} = const.$

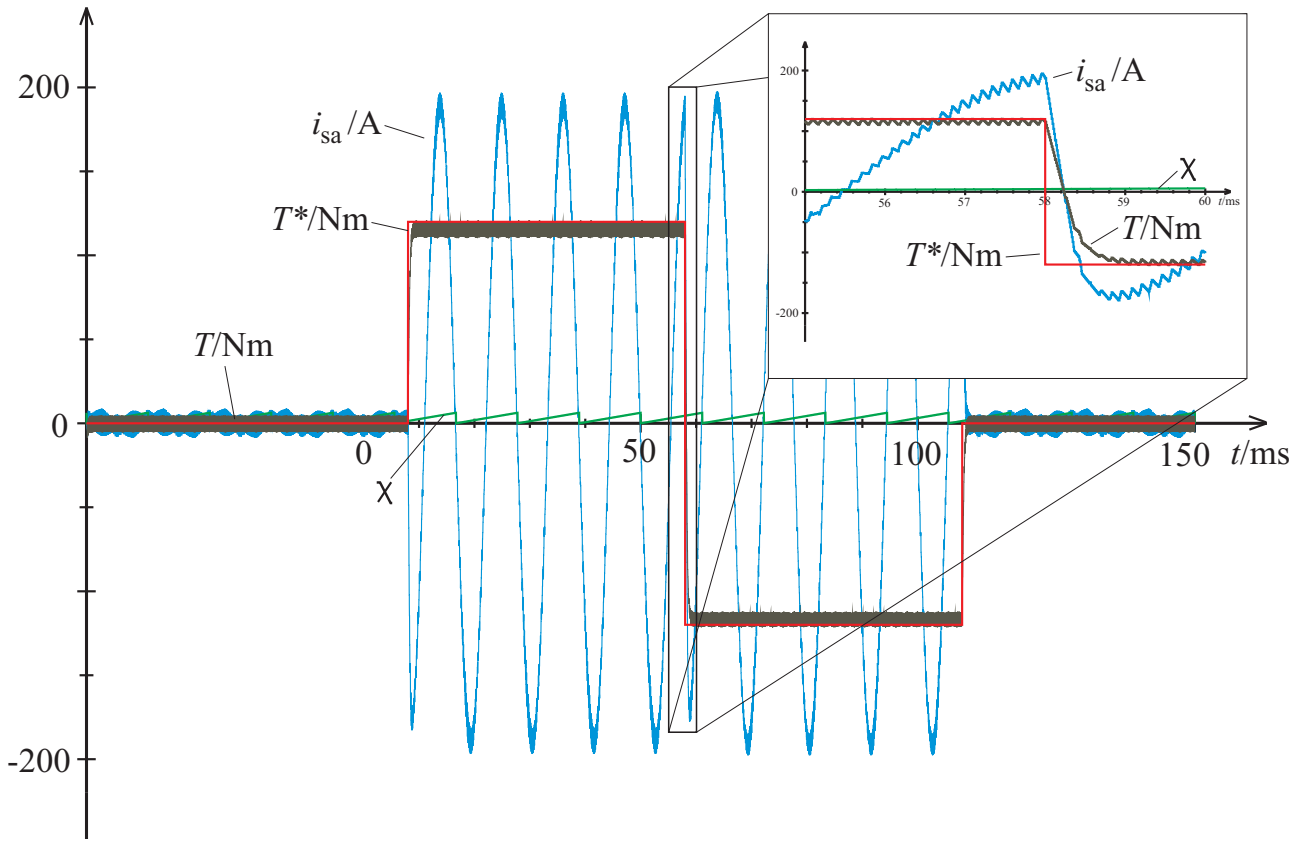


Fig. 9. Torque steps of ISC-controlled PMSM at $n = 900\,\mathrm{min}^{-1}$; $u_{DC} = 200\,\mathrm{V} = const.$